Materials and Design 112 (2016) 124–130

Contents lists available at ScienceDirect

Materials and Design

journal homepage: www.elsevier.com/locate/matdes

Short-range structural and magnetic order in rapidly-solidified Ag—Mn alloys

F. Jiménez-Villacorta [a,b], I. Puente-Orench [c,d], J. Rodríguez-Carvajal [d], L.H. Lewis [a]

[a] Department of Chemical Engineering, Northeastern University, Boston, MA 02115, USA
[b] Instituto de Ciencia de Materiales de Madrid, CSIC, Cantoblanco, 28049 Madrid, Spain
[c] Institut Laue-Langevin, 6 rue Jules Horowitz, 38042 Grenoble, France
[d] Instituto de Ciencia de Materiales de Aragón, CSIC-Universidad de Zaragoza, 50009 Zaragoza, Spain

HIGHLIGHTS

- Fabrication of AgMn alloys with Mn concentration beyond equilibrium (>40 at.%) has been achieved by rapid solidification.
- Identification of two nanocrystalline phases with differing Mn contents refines the compositional fluctuation model.
- Neutron diffraction results confirm the existence of short range structural ordering determining the magnetic character.
- Quantification of tunable interfacial exchange coupling and magnetic anisotropy in this nanocomposite is achieved.

GRAPHICAL ABSTRACT

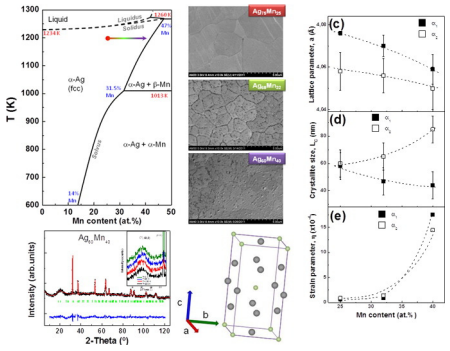

ARTICLE INFO

Article history:
Received 20 June 2016
Received in revised form 6 September 2016
Accepted 18 September 2016
Available online 21 September 2016

Keywords:
Rapid solidification
Melt spinning
Mn-based alloys
Cluster glass
Neutron diffraction
Short range order

ABSTRACT

Short-range structural and magnetic order in rapidly solidified nanostructured $Ag_{100-x}Mn_x$ alloys featuring nominal large Mn content (x = 25, 32, 40 at.%), well above the maximum equilibrium concentration (x ~ 14 at.%), are quantified using X-ray, neutron and magnetic probes. These inhomogenous alloys contain coexisting Mn-rich and Mn-deficient nanoscopic face-centered-cubic-type phases. Interaction between these regions provides large exchange bias at low temperature, with the magnitude of the unidirectional anisotropy field increasing gradually with increased Mn concentration. Neutron diffraction data reveal no evidence of long-range antiferromagnetic ordering but instead identifies short-range structural order from the presence of a diffuse scattering peak that evolves with Mn content. Moderate annealing temperatures (T_{ann} = 350 °C) promote homogenization of the Mn content in the alloys with subsequent suppression of exchange bias, confirming the above model. A strong interfacial exchange density between Mn-deficient and the Mn-rich nanocrystalline phases exists that is determined to be of the same order of magnitude as that found in other exchange-biased ferromagnetic/antiferromagnetic systems. The intriguing behavior of these AgMn alloys as a function of temperature, of Mn content and of annealing condition highlights options to manipulate and tailor their magnetic attributes such as interface exchange and magnetic anisotropy.

1. Introduction

The exchange bias effect that arises from intimate exchange coupling between a ferromagnetic (FM) and an antiferromagnetic (AF) phase [1,2] is a key enabler for the development of spintronic devices [3,4] and may hold promise for application in permanent magnet technology as so-called "exchange-bias" magnets [5,6]. Properly engineered, exchange bias donates enhancements to unidirectional magnetic

http://dx.doi.org/10.1016/j.matdes.2016.09.064
0264-1275/

anisotropy that may stabilize the magnetization [7] to yield improved remanence [8], coercivity [9] and maximum energy product, $(BH)_{max}$ [1,10,11]. Among metallic AF materials, manganese-based binary systems such as Fe—Mn [12], Ir—Mn [13] and Cu—Mn [14] hold potential as components in exchange-biased magnets because their magnetic properties may be tailored by compositional variation [15,16]. However, analogous to the case of exchange-spring nanocomposites [17], incorporation of the anisotropy-donor phase (which is the high-coercivity phase in exchange-spring magnets or the antiferromagnetic phase in exchange-bias magnets) is accompanied by a decrease of the overall magnetization, requiring optimization of the nanocomposite phase volume ratio [18,19]. In this current work, the structural and magnetic properties of $Ag_{100-x}Mn_x$ alloys with Mn concentrations ($25 \le x \le 40$ at.%) retained beyond the equilibrium content are reported. In contrast to equilibrium compositions in the Ag—Mn binary phase diagram with a maximum Mn content of ~14 at.% [20], rapid solidification allows metastable retention of a large fraction of Mn in the Ag—Mn alloys. Solidification of melted alloys by melt spinning is used provides very high cooling rates of up to 10^6 K/s [21]. The quenched Ag—Mn alloys fosters phase separation, chemical disproportionation and a resultant large exchange bias at low temperatures [22]. The origin of such unidirectional anisotropy, recently observed as well in MnAl and Mn-based Heusler melt-spun alloys [23,24,25], resides in fluctuations of Mn content that produces adjacent exchange-coupled nanoscopic regions with predominant FM and AF character.

The Ag—Mn alloys share a rich history with the canonical Au—Mn and Cu—Mn systems [26,27,28] that exhibit spin glass behavior at low temperatures [29,30]. Recently, modified transport and magnetic properties of nanocrystalline AgMn relative to that characterizing it larger-grained counterpart have been observed in alloys of low Mn content [30,31,32]. The seminal work of Morris and Williams [33] on the magnetic susceptibility of AgMn alloys containing Mn up to 38.1 at.%, does not mention exchange anisotropy effects in this system. Kouvel studied AgMn alloys with a moderately enriched Mn content (in the range 11.9 to 23.7 at.% Mn) and identified both spin-glass-like features and exchange bias in these alloys [34,35] that were attributed to the formation FM and AF regions arising from random statistical fluctuations of the Mn content. In every case it has been reported that an increased Mn concentration conveys an increased blocking temperature T_B, defined as the transition temperature between the magnetic spin-glass state and the paramagnetic state, signaled by a cusp in the magnetization *vs.* temperature (*M vs. T*) curves.

This current work reports on magnetic properties and structure of nanocrystalline $Ag_{100-x}Mn_x$ alloys with a high metastable Mn content, $x = 25, 32, 40$ at.%, prepared by melt spinning. Rapid solidification techniques and subsequent quenching yields an increased solid solubility and grain refinement [36]. The interatomic exchange coupling and exchange anisotropy of these alloys are determined to vary systematically with variation in the Mn content. It is envisioned that increased understanding of the tunability of the magnetic features of Mn-based alloys at low temperatures will donate new ideas for increased stability of magnetic media, permanent magnet and exchange-biased magnetic sensor technologies [37,38].

2. Experimental

Silver-manganese ($Ag_{100-x}Mn_x$, $x = 25, 32, 40$ at.%) ribbons were prepared by melt-spinning in an argon atmosphere from pre-alloyed AgMn (99.98% purity) arc-melted charges. During the melt-spinning process, the nozzle-to-wheel distance was fixed at 3 mm and a tangential wheel speed of 31 m/s was employed during the quench. The resultant ductile ribbons possessed thicknesses 50–100 μm and widths of 3–4 mm. The morphology and compositional profile of the quenched ribbons, as well as those of the post-alloyed charges, were evaluated with scanning electron microscopy (SEM) and *in-situ* energy-dispersive X-ray spectroscopy (EDX; Hitachi S-4800). The sample crystallinity and phase constitution were examined by X-ray diffraction (XRD) using Cu-K_α radiation (Philips XPert Pro); lattice parameters were determined using a least-squares cell-parameter fitting program [39]. The average crystallographic grain dimension D and the lattice distortion ratio η, which provides an estimation of the microstrain effects in the lattice, were determined using the Williamson-Hall relationship [40,41] applied to the XRD data:

$$\beta_{total} = \beta_{size} + \beta_{strain} = \frac{k\lambda}{D\cos\theta} + 4\eta\frac{\sin\theta}{\cos\theta} \quad (1)$$

where β_{total} is the full-width at half-maximum of the Bragg diffraction peak, $\eta = \Delta d/d$ is the strain parameter, Δd is the lattice d spacing deviation, k is the Scherrer constant ($k \approx 0.9$), λ is the incident wavelength, and θ is the diffraction angle.

Neutron diffraction experiments were performed in the high-flux two-axis D1B diffractometer at the Institut Laue-Langevin (ILL). Diffraction patterns were collected at selected temperatures from 2 to 300 K using a calibrated wavelength of $\lambda = 1.2899$ Å. The $Ag_{100-x}Mn_x$ ribbons where cut into very small pieces for measurement and were sealed into a 6-mm cylindrical vanadium container that was placed inside a cryostat to control the measurement temperature. The crystal structure was refined by applying the Rietveld method to the data using the FullProf Suite [42].

Magnetic characterization was carried out using a Quantum Design MPMS-5 Superconducting Quantum Interference Device (SQUID) magnetometer. Zero-field cooled-field-cooled (ZFC-FC) magnetothermal curves were measured from in the temperature range $10\ K \le T \le 350$ K under an applied field H_{appl} of 1 kOe. Field-cooled ($H_{appl} = 50$ kOe) and zero-field cooled $M(H)$ loops have been collected at several temperatures in the range 10 K–300 K. The intrinsic coercive field H_{Ci}, defined as the reversal field in the descending branch, the exchange bias field H_E, defined as the average midpoint between the reversal fields of both ascending and descending branches, and the unidirectional anisotropy coefficients were obtained after subtracting the linear contribution of the $M(H)$ loops, following the method of Kouvel [34]. Such experimental linear contribution originates from the linear susceptibility of the antiferromagnetic (cluster-glass) phase (present below the blocking temperature) and the paramagnetic phase (present above the blocking temperature) of the alloys.

Finally, correlations between the magnetic response and the microstructural evolution were investigated in the sample with the composition $Ag_{68}Mn_{32}$ by subjecting it to successive isochronal annealing treatments for 30 min in the temperature range 250–450 °C while vacuum sealed (~10^{-6} Torr) in a 2.5-mm diameter quartz tube to prevent oxidation [43]. The microstructure as well as the magnetic response of the annealed $Ag_{68}Mn_{32}$ sample was routinely examined after every annealing treatment. An experimental process diagram describing the experimental procedure explained above is depicted in Fig. 1.

3. Results

The as-quenched Ag–Mn alloys are confirmed to be homogeneous on the microscale in their as-solidified state (see SEM micrographs in Fig. 2), as rapid solidification may reduce intergrain microsegregation inducing simultaneous extended solid solubility [44,45]. Nevertheless, an increasing roughness and density of small droplets are apparent at the surface with increasing Mn concentration.

X-ray diffractograms of the three samples ($Ag_{100-x}Mn_x$, $x = 25, 32, 40$) in their as-quenched state confirm a predominant face-centered-cubic (*fcc*) α-AgMn phase constitution. Residual contributions of the α-Mn phase to the XRD data appear with increased Mn content. A complex double Bragg-peak structure (see Fig. 3a–b) is observed for all measured peaks. The noted doubling of the major (111) Bragg reflection precludes symmetry lowering as the origin of the double-peak structure. Therefore it is deduced that the as-quenched ribbons consist of